

Construction and performance of a photobleaching recovery apparatus with microsecond time resolution

H. Pin Kao, A.S. Verkman *

Departments of Medicine and Physiology, 1246 Health Sciences East Tower, Cardiovascular Research Institute, University of California, San Francisco, CA 94143-0521, USA

Received 12 July 1995; revised 30 September 1995; accepted 30 September 1995

Abstract

A fluorescence recovery after photobleaching (FRAP) apparatus was constructed to measure sub-millisecond fluorescence recovery processes in living cells. The photobleaching pulse and probe beams were generated by modulating the intensity of a continuous wave Argon laser (4 W) by two acousto-optic modulators in series. The maximum intensity modulation was $> 10^6:1$ with a rise time of $< 1 \mu\text{s}$ and a minimum pulse width of $6 \mu\text{s}$. Fluorescence was detected by a photomultiplier, amplified by a transimpedance amplifier, and digitized at 1 MHz. During the photobleaching pulse, the photomultiplier gain was reduced by ca. 1500-fold by switching the second dynode voltage ca. 100 V negative with respect to the cathode voltage by computer control of two bidirectional Mosfet optoisolators. The switching circuit produced a transient anode current ($\tau \approx 15 \mu\text{s}$) which was subtracted for measurement of recoveries of $< 50\text{--}100 \mu\text{s}$. The apparatus was coupled to an inverted microscope for measurement of fluorescence by epi-illumination or total internal reflection. Instrument performance was evaluated by measurement of the rapid fluorescence recoveries of fluorescein and fluorescein-dextran in solutions and living cells.

Keywords: Fluorimetry; Photobleaching; Cell biology; Membrane biology; Diffusive processes

1. Introduction

Fluorescence recovery after photobleaching (FRAP) has been used extensively in cell and membrane biology to measure the diffusive and directed mobilities of ensembles of fluorescent particles. FRAP experiments have been used to measure the diffusive mobilities of lipids and proteins in biomembranes [1–3] and of fluorescent probes in

aqueous cellular compartments such as cytosol [4,5], and the directed mobility of fluorescently labeled microtubules [6]. Fluorophore mobility is measured from the increase (recovery) in fluorescence signal in an illuminated region after irreversible photobleaching by a brief, intense laser pulse. The time course of fluorescence recovery is dependent upon particle mobility, photobleaching pulse duration, and sample and beam geometry [7]. Several sample and beam geometries for FRAP studies have been reported, such as pattern photobleaching [8] and total internal reflection fluorescence photobleaching (TIR-FRAP [9,10]).

* Corresponding author. Tel.: (415) 476 8530; Fax: (415) 665 3847.

Two major technical requirements of a FRAP apparatus are generating an intense laser pulse (10^3 – 10^5 -fold higher than probe beam intensity) much shorter in duration than the photobleaching recovery half-time ($t_{1/2}$), and a sensitive fluorescence detection system which must be protected during the intense bleach pulse. Many photobleaching recovery systems utilize electromechanical shutters to generate the intense laser pulse and protect the detection system [11]. Because of mechanical limitations, shutters produce a minimum bleach duration of > 1 ms so that diffusive processes faster than ca. 10 ms cannot easily be studied. Moreover, the imperfect alignment of bleach and probe beams in shutter-driven systems potentially complicates the quantitative analysis of recovery curves [7,12,13].

There are a number of biologically important diffusive processes, such as solute diffusion in cytosol, nucleus and mitochondria, which are predicted to generate photobleaching recovery times of < 1 ms in FRAP experiments. Photobleaching of a small fluorophore (diffusion coefficient $\approx 10^{-5}$ cm²/s in water) with a 0.8 μ m diameter spot would give a recovery curve with $t_{1/2}$ of ca. 40 μ s. Because diffusion of a small solute in cell cytosol or nucleus is only retarded ca. 4-fold compared to diffusion in water [5], photobleaching of labeled cells with a small spot would yield recovery times of < 1 ms. Fast recovery times would also be measured in TIR-FRAP studies of aqueous-phase fluorophore diffusion in a 50–200 nm wide evanescent field, such as that required for studies of solute diffusion in membrane-adjacent cytosol. Finally, recovery times for solute diffusion within subcellular organelles, such as mitochondria and Golgi, would be very short because distances for translational diffusion are small. Of course, the ability to observe photobleaching recovery requires that the spot diameter in spot photobleaching studies, or the evanescent field depth in TIR-FRAP, be smaller than the size of the organelle aqueous compartment.

We report here a FRAP apparatus with microsecond resolution bleach times and signal detection. The instrument utilized acousto-optic modulators to vary the intensity of a continuous wave laser beam, and a novel photomultiplier gating circuit to protect the fluorescence detection system during the bleach pulse. The FRAP instrument was evaluated in spot

photobleaching and TIR-FRAP measurements on cell-free fluorophore solutions and fluorescently labeled living cells.

2. Instrument design

The output of a 4-W argon laser (Innova 70-2; Coherent, Palo Alto, CA) was modulated using two acousto-optic modulators (Model OD-8813 AOM with OD-8802 Modular Driver; NEC, Sunnyvale, CA) in series (Fig. 1). The AOMs were positioned to diffract the incoming laser beam maximally into the first order beam. Pinholes (2 mm diameter) were positioned 40 cm beyond the exit of each AOM to isolate first order beams. The first order beam from the second AOM was directed onto the stage of a fluorescence microscope (see below). Each AOM could modulate the intensity of the diffracted laser beam by a factor of $> 10^3:1$, so that beam intensity could be modulated by a voltage-selectable factor of $> 10^6:1$. For most FRAP experiments, the laser beam power was set to 0.1–1 W (488 nm) and the attenuation ratio (the ratio of the bleach beam intensity to the probe beam intensity) was set to 5000–50 000.

Square photobleaching pulses were generated by electronically switching between control voltages supplied to the AOM drivers. A computer-generated TTL signal was used to drive a high-speed analog multiplexer (HI-518-5; Harris Semiconductor, Santa Clara, CA) configured as an analog switch. The selected voltage was buffered using two AD811 high-speed operational amplifiers (one per driver) configured as 50 W line drivers to supply 50 W inputs of the AOM drivers. Data collection was hardware triggered to begin at the falling edge of the AOM control signal. The minimum pulse width achievable with this set-up was 6 μ s with a rise time of < 1 μ s.

Fluorescence was detected by a photomultiplier (9828A; Thorn EMI, Rockaway, NJ) contained in a FACT50 (Thorn EMI) cooled housing. Photomultiplier signals were amplified with a transimpedance amplifier with virtual ground input (Model A1; Thorn EMI) and gain conversion set to either 10^5 V/A (1 μ s rise time) or 10^6 V/A (20 μ s rise time). The output signal was digitized at 1 MHz using a 12–14

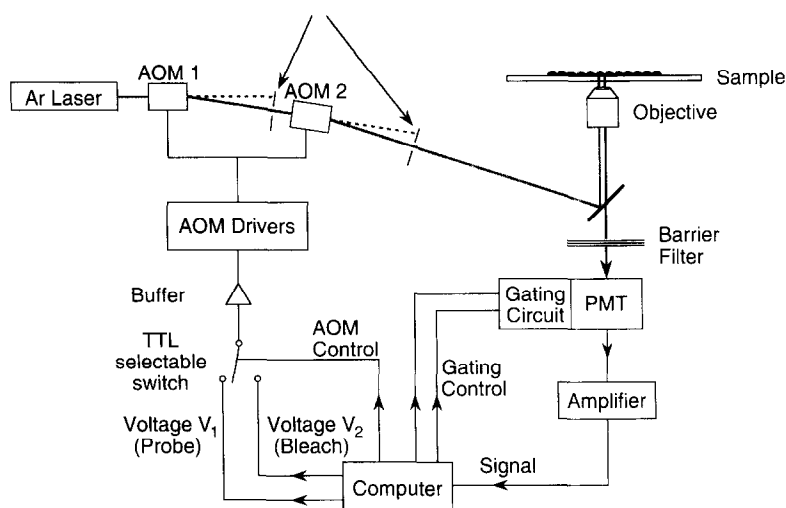


Fig. 1. Schematic of the photobleaching recovery apparatus. The beam from a continuous-wave Ar laser was modulated by two acousto-optic modulators (AOM1 and AOM2) and directed onto the stage of a fluorescence microscope configured here for epi-illumination. The computer sets probe (V_1) and bleach (V_2) voltages to drive the AOMs, activates the photomultiplier protection circuit (gating circuit), and digitizes the amplified photomultiplier anode current. See text for details.

bit analog-to-digital converter (Flash 12, Model 1; Strawberry Tree, Santa Clara, CA). Control pulses were generated using a precision microsecond timing

board (PC-TIO-10; National Instruments, Austin, TX).

During the photobleaching pulse, a gating circuit

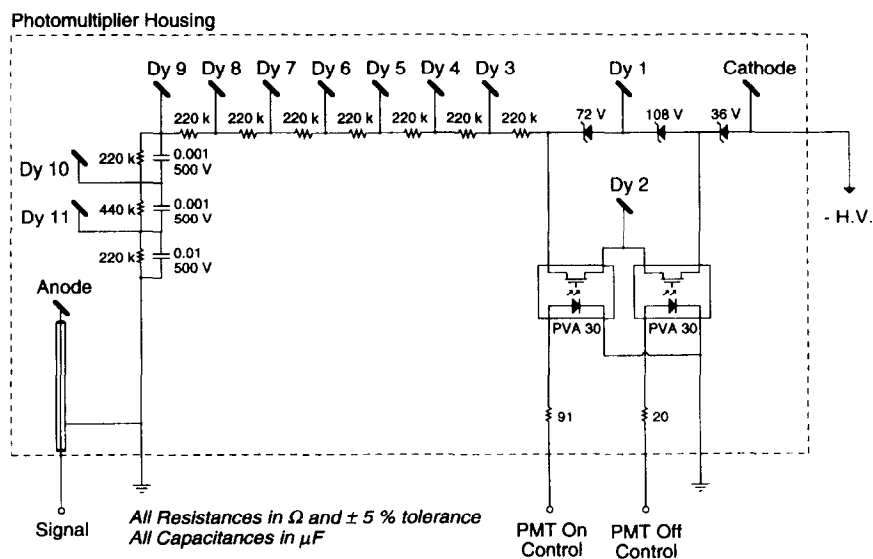


Fig. 2. Photomultiplier gating circuitry. Computer-generated control pulses set the voltage on dynode 2. Bidirectional Mosfets were used to isolate control voltages from photomultiplier high voltage. The circuit was mounted directly on the photomultiplier connection socket located within the shielded housing. See text for details.

was used to transiently decrease photomultiplier gain for protection against damage or overload (Fig. 2). The gating circuit was activated at 2 μ s before the photobleaching pulse and deactivated at 3 μ s after the pulse. The circuit switched the second dynode of the photomultiplier between its normal operating voltage and 108 V more negative than the first dynode. Zener diodes were utilized to clamp the two voltage levels in order to minimize the sensitivity of transient anode currents to photomultiplier voltage. Anode connections within the photomultiplier housing were shielded to reduce capacitive transient anode switching currents. Two bidirectional Mosfets (PVA30, International Rectifier) were configured to set the second dynode voltage. These components optically isolated the computer control signals from the photomultiplier high voltage, and responded rapidly without the need for an external floating power supply. The gain of the photomultiplier was reduced by ca. 1500-fold during the off state. The transient currents detected at the anode were subtracted from measured recovery curves.

Software was written in Microsoft QuickBasic 4.5 to record pre-bleach and post-bleach signals over specified time intervals, and to modulate the laser beam intensity and activate the photomultiplier protection circuitry during photobleaching. Signals were sampled prior to the bleach (generally 10^3 data points over 100 ms), and over three different time intervals after the bleach: high-resolution data (10^3 – 10^5 points) over ca. $4t_{1/2}$ intervals, low-resolution data (generally 10^4 points) over ca. $20t_{1/2}$ intervals, and “final signal” data (10^3 points) at time ca. $100t_{1/2}$. High- and low-resolution data were generally binned into 200 points each for storage and analysis. Half-times ($t_{1/2}$) for fluorescence recovery were determined from bi- or tri-exponential least-squares fits of recovery curves.

3. Methods

Solution preparation. Solutions of 1 mM fluorescein were prepared in phosphate-buffered saline (PBS), pH 8.0, containing specified glycerol concentrations. Glycerol content was measured by optical refractometry and solution viscosity was determined from the CRC Handbook of Chemistry and Physics.

FRAP measurements were performed on 2–10 μ m thicknesses of solutions prepared by sandwiching evenly spread films of fluorescein-containing solutions between two fused silica coverslips.

Cell culture and labeling. Swiss 3T3 fibroblasts (ATCC CL-101) were grown on 10 mm diameter round fused silica coverslips in DME-H21 medium supplemented with 5% fetal calf serum at 37°C in a 95% air–5% CO₂ incubator. Cells were used just before confluence. Cell nucleus was loaded with fluorescein isothiocyanate (FITC)–dextran (150 kDa, Molecular Probes) by single cell microinjection [14]. Cells were washed and mounted in a perfusion chamber in which the cell-free coverslip surface was accessible to short working distance objectives.

Fluorescence microscopy. The laser beam was directed onto the stage of a Nikon inverted fluorescence microscope (Diaphot) for spot photobleaching or TIR-FRAP. For epi-illumination, the 488 nm beam was reflected off of a 510 nm dichroic mirror and focused with an objective lens (25 \times dry, NA 0.35, Leitz; \times 40 quartz glycerol, NA 0.65, Leitz; 60 \times or 100 \times oil plan-apo, NA 1.4, Nikon). For TIR-FRAP, the beam was directed at a subcritical angle onto a right triangular quartz prism (8 mm edge) which was optically coupled (by glycerol) to the cell-free surface of the coverslip [15]. A 25 \times objective (working distance 24 mm, Leitz) was positioned proximal to the prism to focus the beam to a small spot at the quartz–aqueous interface. Unless otherwise indicated, emitted fluorescence was filtered by a 530 ± 15 nm interference filter and detected by the gated photomultiplier as described above.

4. Instrument performance

Fig. 3 shows performance characteristics for the FRAP instrument. The response time of the AOMs was determined by direct measurement of beam intensity without photomultiplier gating. Photomultiplier current responded rapidly to a small square voltage pulse driving the AOMs (Fig. 3A). The $t_{1/2}$ value for the rise and fall of the anode current was 300–600 ns, and insensitive to illumination intensity and AOM control voltage levels.

The efficiency and response of the photomultiplier protection circuit was next examined. The gat-

ing circuit extinction ratio is defined as the ratio of photomultiplier gain with the protection circuit activated to that with the circuit inactivated. Fig. 3B shows the anode current first with the protection circuit activated during intense illumination, and then with the protection circuit inactivated and illumination intensity decreased by 3400-fold. Inactivation of the protection circuit produced a brief transient anode current observed as a downward deflection (see below). The ratio of averaged anode current with the protection circuit activated to that with the circuit inactivated was 0.44, giving an extinction ratio of ca. 1500.

In response to a square gating control pulse in the absence of illumination, the anode current showed a biphasic transient response with a negative anode current over ca. 15 μs (Fig. 3C, top). Further analysis indicated that the transient anode current was due to capacitive coupling of electrodes within the photomultiplier (anode, cathode and dynodes), and not to amplifier overload or circuit response time. The transient anode current was relatively insensitive to illumination intensity as demonstrated by the response to gating a pulse applied during constant non-zero photomultiplier illumination (Fig. 3C, bottom). The transient anode current could thus be subtracted for measurement of very fast recovery processes.

Applications of the FRAP apparatus to measure rapid recoveries in solutions and intact cells are shown in Fig. 4. Several phenomena were detected that cannot be observed with millisecond bleach and detection times. After a brief bleach pulse, very rapid fluorescence recoveries ($t_{1/2} \approx 10\text{--}100\ \mu\text{s}$) were detected for fluorophores in solutions of high viscosity. Fig. 4A shows the fluorescence recovery after photobleaching of fluorescein in 90% glycerol with $t_{1/2}$ of 58 μs . This recovery process was independent of beam diameter ($\times 20\text{--}\times 100$ objectives), indicating that it does not arise from macroscopic fluorophore diffusion from the unbleached to the bleached zone. Based on additional experiments, it was concluded that this phenomenon arises from reversible photobleaching involving triplet state cross-over [18]. Another observation in sub-millisecond FRAP measurements was the appearance of a large positive recovery process in some experiments as seen in Fig. 4B. The amplitude of the positive deflection was proportional to bleach intensity, independent of solution

composition and probe beam intensity (intensity set to zero in Fig. 4B), and occurred at wavelengths higher than the fluorophore emission maxima. This process was found to be phosphorescence from glass coverslips. Replacement of glass with quartz eliminated completely the positive signal.

The FRAP apparatus was applied to study diffusive recovery processes that are too fast to detect with millisecond bleach and detection times. Fig. 3C shows a photobleaching recovery study of fluorescein in an aqueous buffer obtained with TIR illumination. The laser illumination angle was 68.4° , giving an exponentially decaying evanescent field with distance constant of ca. 150 nm. The recovery was remarkably non-exponential, increasing by 50% with $t_{1/2} \approx 180\ \mu\text{s}$ and at a slower rate thereafter. The rapid recovery process was not observed with supercritical (trans) illumination and was dependent upon solution viscosity and laser beam illumination angle. The recovery thus represents one-dimensional move-

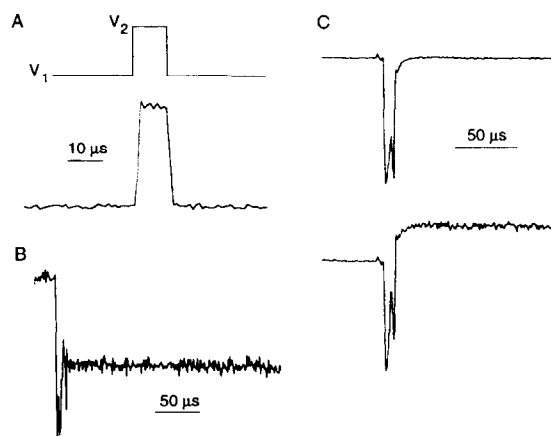


Fig. 3. Response characteristics of the FRAP apparatus. (A) Modulation of laser beam intensity by serial AOMs. AOMs were gated to diffract incident light into the first order (gating voltages: $V_1 = 1.0$ and $V_2 = 1.1$ V). Photomultiplier anode current response is shown. (B) Extinction ratio of photomultiplier protection circuit. Anode current was monitored with gating circuitry activated (during illumination at high intensity) and then with the gating circuitry off (illumination intensity decreased 3400-fold). A solution of 1 mM fluorescein in 90% glycerol–10% PBS was epi-illuminated to generate the fluorescence signal. Extinction ratio was 1470. (C) Transient anode current in response to photomultiplier gating shown without illumination (top) and with moderate illumination turned on at the time of the bleach pulse (bottom).

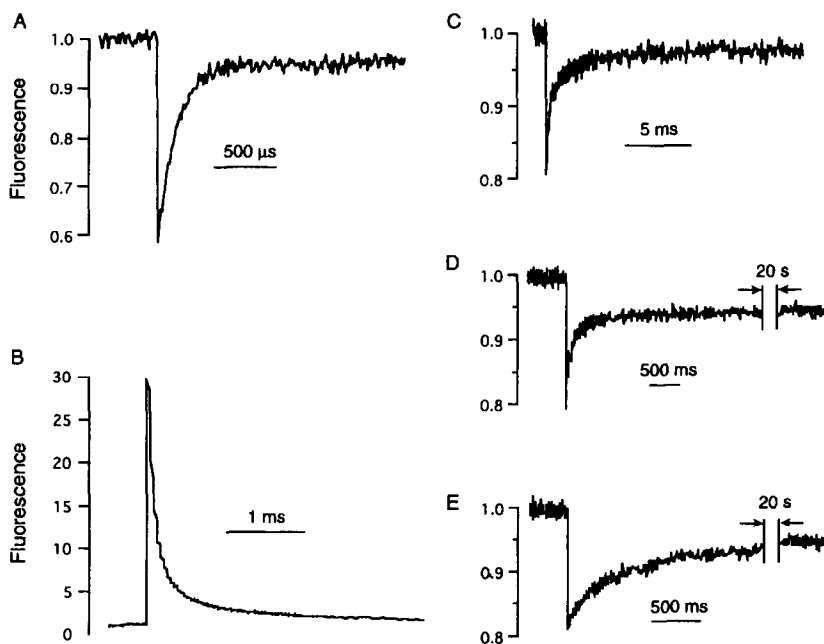


Fig. 4. FRAP measurements in solutions and Swiss 3T3 fibroblasts. (A) Reversible photobleaching of a 20 μm film of 0.5 mM fluorescein in 90% glycerol–10% PBS. Bleach pulse duration was 10 ms. (B) Phosphorescence of a glass coverslip (BK7 glass) measured with a 100 μs "bleach pulse" after which time the illumination intensity was decreased by 10^6 -fold. Phosphorescence was filtered by a 515 nm cut-on filter. (C) TIR-FRAP measurement of 1 mM fluorescein in 30% glycerol–70% PBS. Bleach duration was 25 μs and beam illumination angle (quartz right angle prism) was 68.4° (critical angle 63.5°). (D) FRAP measurement of BCECF-loaded Swiss 3T3 fibroblasts using a $\times 25$ objective by epi-illumination with 100 μs bleach pulse duration. (E) FRAP measurements of 3T3 fibroblasts microinjected with 150 kDa FITC–dextran carried out as in D.

ment of unbleached dye from out of the TIR evanescent field to within the evanescent field detection zone. This represents the first demonstration of TIR-FRAP of diffusive solute movement in solution.

FRAP studies in living Swiss 3T3 fibroblasts are shown in Fig. 4D and E. We showed previously that translational diffusion of the small polar solute bis-2-carboxymethyl-5-carboxyfluorescein acetoxymethyl ester (BCECF) in cytoplasm was slowed ca. 4-fold compared to that measured in aqueous buffers [5]. Fig. 4D shows the fluorescence recovery from BCECF in the cell nucleus. Fluorescence recovered to ca. 80% of its initial level with a $t_{1/2}$ of ca. 65 ms. This data suggests that the effective viscosity of the fluid phase of cell nucleus is similar to the viscosity of cytoplasm. Fig. 4E shows the recovery from a large (150 kDa) FITC–dextran microinjected into the cell nucleus. Fluorescence recovered to ca. 85% of its initial level with a $t_{1/2}$ of ca. 600 ms,

indicating remarkably slowed diffusion compared with BCECF.

5. Discussion

A photobleaching recovery apparatus was constructed to study rapid photochemical and diffusive processes which yield sub-millisecond recovery times. Two acousto-optic modulators in series generated a brief intense bleach pulse, and novel gating circuitry attenuated photomultiplier gain during the bleach pulse. A transient anode current was produced by photomultiplier gating and subtracted for measurement of recovery processes of under ca. 100 μs . For relatively bright samples, recovery curves of under 50 μs were easily detected; measurable recovery times can be reduced further by signal averaging and photon counting signal detection.

Acousto-optic modulators were selected for beam

intensity modulation because of their rapid response, high light transmittance, and simple optical alignment, as first proposed by Garland [16]. An important design criteria in the design of a FRAP instrument is the ability to generate square photobleaching pulses of short duration. In early FRAP instruments, the attenuated beam was formed by rapidly (ca. 100 ms) removing and reinserting a neutral density filter in the beam path. Many present FRAP devices use manual or electromechanical shutters to modulate laser beam intensity [11]. In these instruments, the laser beam is split into an intense bleach beam and an attenuated probe beam, and the two beams are recombined by beam-splitting optics. A computer-controlled shutter is positioned in the bleach beam to produce the photobleaching pulse. However, the rise time of these shutters (ca. 1 ms) limit their ability to study very fast recovery processes. Moreover, it is difficult to obtain precise overlap of bleach and probe beams in the sample plane, which can affect the kinetics of photobleaching recovery [12]. In contrast to these methods, AOMs can produce a rapid square photobleaching pulse (ca. 3 μ s) with little light loss and without the need for beam alignment. In a previous report [13], a single AOM was used to modulate beam intensity in a polarization FRAP apparatus, although photomultiplier protection was not required because relatively small attenuation ratios were used. Electro-optic modulators are another possible method for beam modulation in a FRAP apparatus [11]. However, although electro-optic modulators can have a rapid response and high light transmittance, high-voltage drivers and polarization optics are required.

The main challenge in the construction of the FRAP apparatus was design of the photomultiplier protection circuit. Without protection, the unattenuated laser beam would saturate various photomultiplier and amplifier components which would produce long-lived transient signal artifacts, as well as possible irreversible damage to the photomultiplier photocathode. After evaluating various gating strategies, including grounding the fifth anode and reverse biasing the cathode, the present scheme of modulating the voltage on the second dynode was selected. Capacitive anode current transients are in general unavoidable for any gating technique which sets anode or dynode voltages. The size and duration of

the transient anode current is dependent upon dynode geometry, dynode voltages, and gating circuit specifications. Switching the voltage at the cathode or first dynode generated large transients because of the large surface of the cathode. Switching the fifth dynode did not attenuate the photomultiplier gain efficiently. The gating circuit voltages chosen generated a minimum anode current transient and produced a high extinction ratio. If a high extinction ratio is not required for studies utilizing less intense photobleaching pulses, then the configuration of the photomultiplier gating circuit clamp voltages can be modified (by diode replacement) to reduce further the transient anode current. Possible alternative detectors for fast photobleaching measurements include a high-sensitivity avalanche photodiode, or a photomultiplier having a gating electrode between the photocathode and first dynode.

There are several technical concerns for FRAP studies of sub-millisecond diffusive processes. The intense photobleaching pulse may excite phosphorescence in instrument components, such as certain glasses (Fig. 4B), and in various solution constituents. Apparent "reversible photobleaching" [17,18], resulting from cross-over between singlet and triplet energy levels, may be observed as an apparent fluorescence signal recovery on sub-millisecond time scales even in the absence of fluorophore diffusion (Fig. 4A). Reversible photobleaching is of greater concern under anoxic conditions, and with fluorophores having low fluorescence quantum yield. Finally, the signal-to-noise ratio in sub-millisecond FRAP measurements may be marginal because of the wide amplifier bandwidth required for detection of rapid signals. Signal-to-noise can be optimized by use of suitable optical and detection components, signal averaging, and photon counting detection. Notwithstanding these concerns, the results here demonstrate that sub-millisecond FRAP measurements are possible with our instrument and should provide useful information about fluorophore photochemistry and solute diffusion within living cells.

Acknowledgements

We thank Dr. Steve Bicknese for assistance in the cell and TIR-FRAP measurements and Dr. Olivier

Seksek for intracellular microinjections. This work was supported by grant DK43840 from the National Institutes of Health.

References

- [1] S. Ladha, A.R. Mackie and D.C. Clark, *J. Membrane Biol.*, 142 (1994) 223–228.
- [2] D.A. Berk and R.M. Hochmuth, *Biophys. J.*, 61 (1992) 9–18.
- [3] K. Jacobson, A. Ishihara and R. Inman, *Annu. Rev. Physiol.*, 49 (1987) 163–175.
- [4] K. Luby-Phelps, P.E. Castle, D.L. Taylor and F. Lanni, *Proc. Natl. Acad. Sci. USA*, 84 (1987) 4910–4913.
- [5] H.P. Kao, J.R. Abney and A.S. Verkman, *J. Cell Biol.*, 120 (1993) 175–184.
- [6] J.M. Hush, P. Wadsworth, D.A. Callahan and P.K. Hepler, *J. Cell Sci.*, 107 (1994) 775–774.
- [7] A. Lopez, L. Dupou, A. Altibelli, J. Trotard and J.F. Tocanne, *Biophys. J.*, 53 (1988) 963–970.
- [8] K. Jacobson, F. Zhang and T.T. Tsay, *Scanning Microsc.*, 5 (1991) 357–362.
- [9] H.V. Hsieh and N.L. Thompson, *Biophys. J.*, 66 (1994) 898–911.
- [10] A.L. Stout and D. Axelrod, *Biophys. J.*, 67 (1994) 1324–1334.
- [11] D.E. Wolf, *Methods Cell Biol.*, 30 (1989) 271–306.
- [12] B.G. Barisas, *Biophys. J.*, 29 (1980) 545–548.
- [13] M. Velez and D. Axelrod, *Biophys. J.*, 53 (1988) 575–591.
- [14] O. Seksek, J. Biwersi and A.S. Verkman, *J. Biol. Chem.*, 270 (1995) 4967–4970.
- [15] S. Bicknese, N. Periasamy, S.B. Shohet and A.S. Verkman, *Biophys. J.*, 65 (1993) 1272–1282.
- [16] P. Garland, *Biophys. J.*, 33 (1981) 481–482.
- [17] B.A. Scalettar, P.R. Selvin, D. Axelrod, M.P. Klein and J.E. Hearst, *Biochemistry*, 29 (1990) 4790–4798.
- [18] N. Periasamy, S. Bicknese and A.S. Verkman, *Photochem. Photobiol.*, (1996) in press.